CHEMISTRY
A European Journal

A Journal of
ChemPubSoc Europe

Accepted Article

Title: Visible Light Mediated Liberation and in situ Conversion of Fluorophosgene

Authors: Daniel Petzold, Philipp Nitschke, Fabian Brandl, Veronica Scheidler, Bernhard Dick, Ruth M. Gschwind, and Burkhard König

To be cited as: *Chem. Eur. J.* 10.1002/chem.201804603

Link to VoR: http://dx.doi.org/10.1002/chem.201804603

Supported by
ACES

WILEY-VCH

10.1002/chem.201804603

WILEY-VCH

Visible Light Mediated Liberation and *in situ* Conversion of Fluorophosgene

Daniel Petzold[¶], Philipp Nitschke[¶], Fabian Brandl, Veronica Scheidler, Bernhard Dick, Ruth M. Gschwind, and Burkhard König*[a]

Abstract: *We report the first example for the photocatalytic generation of a highly electrophilic intermediate that is not based on radical reactivity. The single electron reduction of bench stable and commercially available 4-(trifluoromethoxy)benzonitrile by an organic photosensitizer leads to its fragmentation into fluorophosgene and benzonitrile. The in-situ generated fluorophosgene was used for the preparation of carbonates, carbamates and urea derivatives in moderate to excellent yields via an intramolecular cyclization reaction. Transient spectroscopic investigations suggest the formation of a catalyst charge-transfer complex-dimer as the catalytic active species. Fluorophosgene as a highly reactive intermediate, was indirectly detected via its next downstream carbonyl fluoride intermediate by NMR. Furthermore, detailed NMR analyses pro-vided a comprehensive reaction mechanism including a water de-pendent off-cycle equilibrium.*

Introduction

Carbonates, carbamates and urea derivatives are privileged structures in organic synthesis and common motifs in pharmaceuticals, pesticides and plastics (Fig. 1a).[1] Many methods for the synthesis of these compounds have been described.[2] The direct and most hazardous way is the use of gaseous phosgene or its less reactive derivatives diphosgene and triphosgene.[3] However, handling of those compounds in the lab or in industry plants requires special safety precautions due to their severe toxicity.[4] Alternative procedures utilize activated or non-activated carbonates or ureas, which are either prepared by reaction with phosgene or less efficiently from CO_2 (Fig. 1b).[2a, 5] Some of these procedures require harsh reaction conditions or suffer from low reactivity and poor atom economy.[2] Therefore, there is still a significant demand for a less hazardous, practical and easily controllable generation of reactive C1 building blocks. Photoredox catalysis with organic photosensitizers has received tremendous attention in the past years.[6] Many useful transformations without the need of metal catalysts were discovered, exploiting the versatile reduction and oxidation potentials of organic photocatalysts.[7] The common requirement for a typical photocatalytic reaction is the generation of a radical species which can either react with another radical, a sp^2/sp center, a nucleophile or a metal complex.[8] However, the photocatalytic generation of intermediates with pure ionic reactivity remains elusive because energy and single electron transfer are the predominant reaction paths of all common photocatalysts.[9] But especially under photo-reductive conditions most leaving groups are ionic species, e.g. halides, pseudo halides or cyanide, which are neglected in the course of the reaction because they possess only limited reactivity and/or were already exploited in thermal and photochemical reactions (Fig. 1c).[10] On the other hand, the C-OCF_3 bond could only be activated electrochemically or under harsh reaction conditions so far.[11] However, the photocatalytic N-OCF_3 cleavage of complex starting materials was reported very recently.[12] To address the need of a hazard- and metal-free access to highly reactive C1 building blocks, we envisioned to cleave the C-OCF_3 bond of a simple, commercially available aryl trifluoromethoxy ether by photoredox catalysis. We identified 4-(trifluoromethoxy)-benzonitrile as a suitable starting material, which can be cleaved quantitatively into benzonitrile and fluorophosgene by an organic photosensitizer (Fig. 1d). Furthermore, we investigated the reaction mechanism by NMR kinetic and structural analyses and propose a photo-reductive mechanism based on the results of radical trapping experiments and excited state quenching experiments monitored by transient spectroscopy.

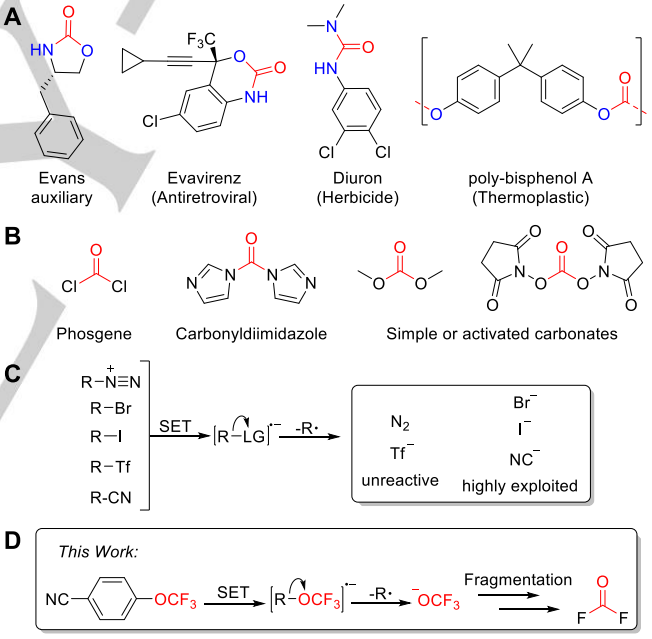

Figure 1. a) Structures of prominent carbamate or urea containing molecules used in synthesis, pharmacy, agriculture and daily life. **b)** Structures of phosgene and commonly employed alternatives. **c)** Typical leaving groups and their reactivity profile in photoredox catalysis. **d)** Overview of the photocatalytic fluorophosgene generation; Tf = trifluoromethanesulfonate, R = benzonitrile.

Results and Discussion

We began our investigation using 2-benzylaminoethanol (**1a**) as a model substrate, Rhodamine 6G (**P1**) as a strongly reducing photosensitizer, diisopropylethylamine (DIPEA) as electron donor and trifluoromethoxybenzene (**2a**) as fluorophosgene precursor in neat acetonitrile.[14] However, no conversion of **2a** was observed (Table 1 entry 1). Switching to commonly employed $Ir(ppy)_3$ (**P2**) or to the recently reported, phenoxazine based photosensitizer **P3** did also not lead to fragmentation of **2a** (entries 2-3).[13] Therefore, trifluoromethoxybenzene derivative **2b** bearing an electron withdrawing nitrile group was employed.

[a] D. Petzold, P. Nitschke, F. Brandl, V. Scheidler, Dr. B. Dick, Dr. R. M. Gschwind, Dr. B. König
Institut für Organische Chemie
Universität Regensburg
Universitätsstrasse 31, Germany
Burkhard.Koenig@chemie.uni-regensburg.de

Hence, the redox potential of **2b** was much more accessible (E_{red}(**2a**) = -3.0 V vs. SCE compared with E_{red}(**2b**) = -2.1 V vs. SCE, see Fig. S1) and **2b** showed slow conversion in the presence of photosensitizer **P2** (entry 4). The reaction was significantly improved by switching to **P3** giving full conversion of **2b** and **1** (entry 5). Further optimization of the reaction lead to conditions giving **3a** in an excellent isolated yield (entry 6). Control experiments revealed that without catalyst, light or DIPEA no or only trace amounts of product could be obtained (entries 7-9). Finally, we observed that the cleavage of **2b** was independent of the presence of **1** (entry 10).

Table 1. Optimization of the reaction conditions

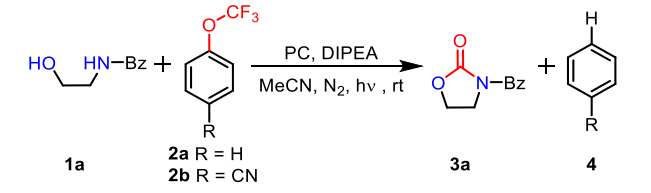

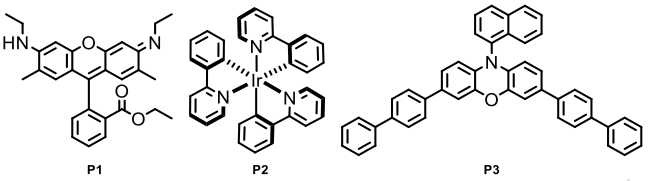

Entry	PC (mol%) / λ	Conversion of 2a/2b[a]	Conversion of 1a[a]
1	**P1** (10) / 455 nm	**2a** 0%	0%
2	**P2** (2) / 455 nm	**2a** 0%	0%
3	**P3** (5) / 400 nm	**2a** 0%	0%
4	**P2** (2) / 455 nm	**2b** 51%	40%
5	**P3** (5) / 400 nm	**2b** 100%	100%
6[b]	**P3** (2) / 400 nm	**2b** 100%	100% [96%]
7[b]	400 nm	**2b** 0%	0%
8[b, c]	**P3** (2)	**2b** 0%	0%
9[b, d]	**P3** (2) / 400 nm	**2b** traces	traces
10[b, e]	**P3** (2) / 400 nm	**2b** 100%	0%

General conditions: A mixture of 0.1 mmol of **1a**, 2 eq. of **2b**, the indicated amount of PC, 4 eq. of DIPEA in neat MeCN (0.1 M) under N_2 atmosphere were irradiated for 24 h with 400 nm light (or 455 nm for **P1** and **P2**). **a**: Conversion determined by GC-FID, isolated yield of **3a** in brackets. **b**: A mixture of 0.1 mmol of **1a**, 1.05 eq. of **2b**, 2 mol% **P3**, 3 eq. of DIPEA in dry MeCN (0.1 M) under N_2 atmosphere were irradiated for 24 h at 400 nm. **c**: no light, 48 h. **d**: no DIPEA. **e**: no **1a**. Bz = benzyl.

In the next step, the synthetic scope of the method was investigated (Scheme 1). *N*-substituted, five membered cyclic carbamates and ureas were prepared in good to excellent yield (Fig. 2, **3b**-**3d**). Unsubstituted, five and six membered cyclic carbamates, carbonates and ureas also showed good to excellent conversion (**3e**-**3j**). More complex carbamate **3k** was isolated in good yield with a diastereomeric ratio of 1:1. 1,2-Cis-configured carbamate **3l** and carbonate **3m** were prepared in moderate to good yield without racemization. Subsequently, amino acids and amino alcohols were investigated. The ethyl and benzyl ester of serine (**3n** and **3o**), as well as the methyl ester of threonine (**3p**) gave good to excellent yields. Noteworthily, **3p** was obtained diastereomerically pure indicating that no racemization of the reactive α-position took place. The methyl ester of cysteine (**3q**) gave a moderate yield, but demonstrated that also thiocarbamates can be obtained by this method. The corresponding carbamates of the amino alcohols prolinol, valinol and tyrosinol were isolated in moderate yields (**3r**-**3t**), whereas tryptophanol and methioninol showed good to excellent conversion to **3u** and **3v**, respectively. Finally, some bioactive compounds were subjected to this method. Uridine and ribothymidine as well as the antiviral drug ribavirin were converted to **3w**, **3x** and **3y** with low to moderate yields. Finally, the beta-blocker propranolol, the neurotransmitter adrenalin and the sympathomimetic ephedrine gave good yields of the cyclized products (**3z**-**3ab**). To demonstrate the synthetic utility of the reaction, a gram scale reaction, using **1a** as substrate, was performed. The corresponding product **3a** was isolated with 70% yield after a prolonged reaction time of 48 h.

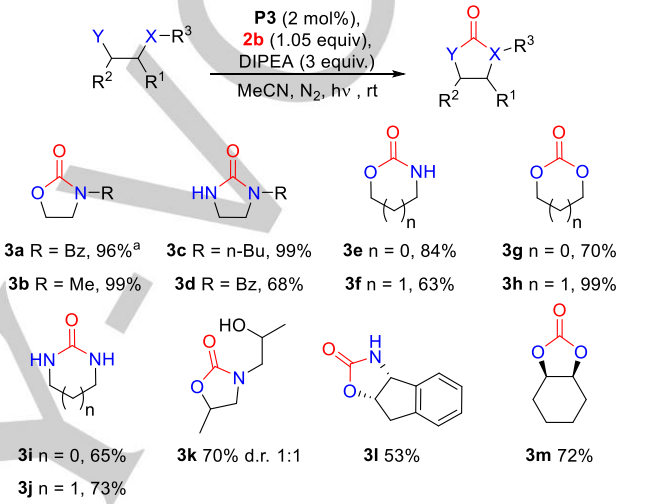

Amino acids and amino alcohols

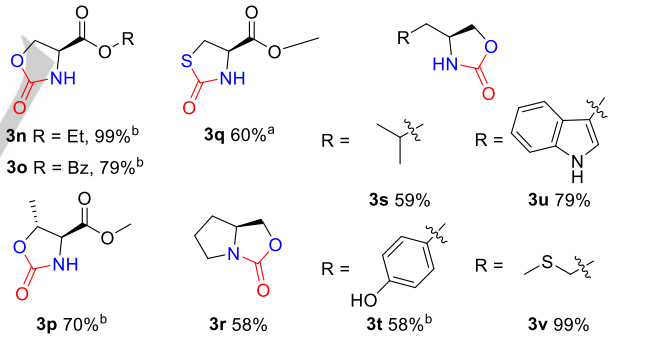

Bioactive compounds

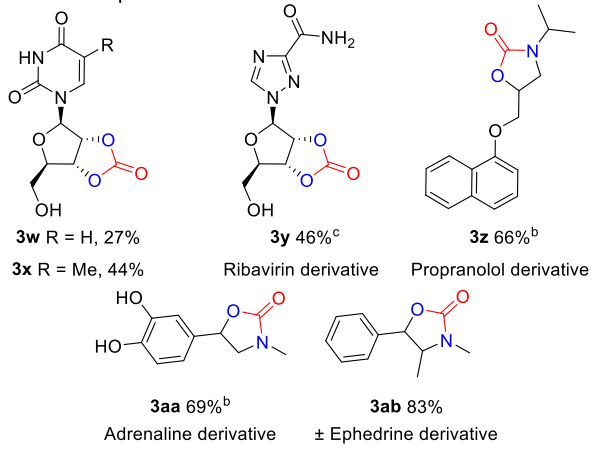

Scheme 1. General conditions: A mixture of 0.1 mmol of substrate, 1.05 eq. of **2b**, 2 mol% **P3**, 3 eq. of DIPEA in neat MeCN (0.1 M) under N_2 atmosphere were irradiated for 24 h with 400 nm light. **a**: 70% isolated yield on a 7 mmol (gram)scale. **b**: 4 eq. of DIPEA were used because the starting material was a hydrochloride salt. **c**: DMF (0.1 M) was used as the solvent. Bz = benzyl, Me = methyl, n-Bu = n-butyl, Et = ethyl.

To investigate the mechanism, transient spectroscopy, cyclovoltammetry as well as radical trapping experiments and *in-situ* and *ex-situ* NMR analyses were performed. To get insight into the photocatalytic mechanism, the quenching of the excited state of **P3** was investigated by transient spectroscopy. The measurements revealed that both, addition of DIPEA (E_{ox} = +0.8 V vs. SCE) and **2b** (E_{red} = -2.1 V vs. SCE) had no influence on the triplet lifetime of **P3** (E_{ox} = +0.4 V; E_{red} = -1.7 V, see Fig. S2).[14] However, during measurements at catalyst concentrations of 30 µM and above (compared to 2 mM under the reaction conditions), we observed a charge-transfer band originating from the radical cation part in the catalyst CT-complex dimer.[15] The lifetime of this band decreases significantly by addition of DIPEA (Fig. 2a). This indicates, that the charge recombination might be slowed down by interaction of the radical cation part of the CT-complex with DIPEA. As a consequence, the radical anion part can reduce **2b** to restore its uncharged ground state. This assumption is supported by cyclovoltammetry of **P3** revealing a ground state reduction potential of the **P3** radical anion of about -2.5 V vs. SCE in MeCN (see Fig. S1 and see SI for more data about the mechanistic investigation). Currently, further transient spectroscopic investigations on **P3** and this catalytic transformation are ongoing in our lab.

To find evidence for the presence of a benzonitrile radical originating from a photo-reductive mechanism, we performed radical trapping experiments in presence of **1a**. We observed 48% conversion of **2b** to the corresponding *N*-methylpyrrole adduct **5a** (Fig. 2b). Moreover, the aryl radical could be trapped with the isolated double bond of allylbenzene giving adduct **5b** in 45% yield. The different radical trapping conditions did not influence the conversion of **1a** significantly, as **3a** was isolated in high yields. The formation of **5a** and **5b** is a good indication for the intermediacy of an aryl and the operation of a photo-reductive mechanism.[16] *In-situ* ^{1}H and ^{19}F NMR profiles further corroborate this mechanistic step monitoring a clean transformation of **2b** into **4** upon illumination of **P3** in the presence of DIPEA (see Fig. S16 and S18). Next, an *ex situ* NMR profile of the whole reaction with substrate **1a** was recorded (Fig. 2c). Upon illumination, **2b** (black) and **1a** (violet) start to decrease, while the two main products **3a** (green) and **4** (red) can be readily detected. Furthermore, two more reaction intermediates could be identified (**F-I**, magenta and **OC-I**, cyan). Instead of the highly reactive free fluorophosgene itself, the formation of its next downstream more stable reaction intermediate (**F-I**) with **1a** was observed. Using advanced 1D and 2D NMR techniques for the ^{1}H, ^{19}F and ^{13}C assignment the

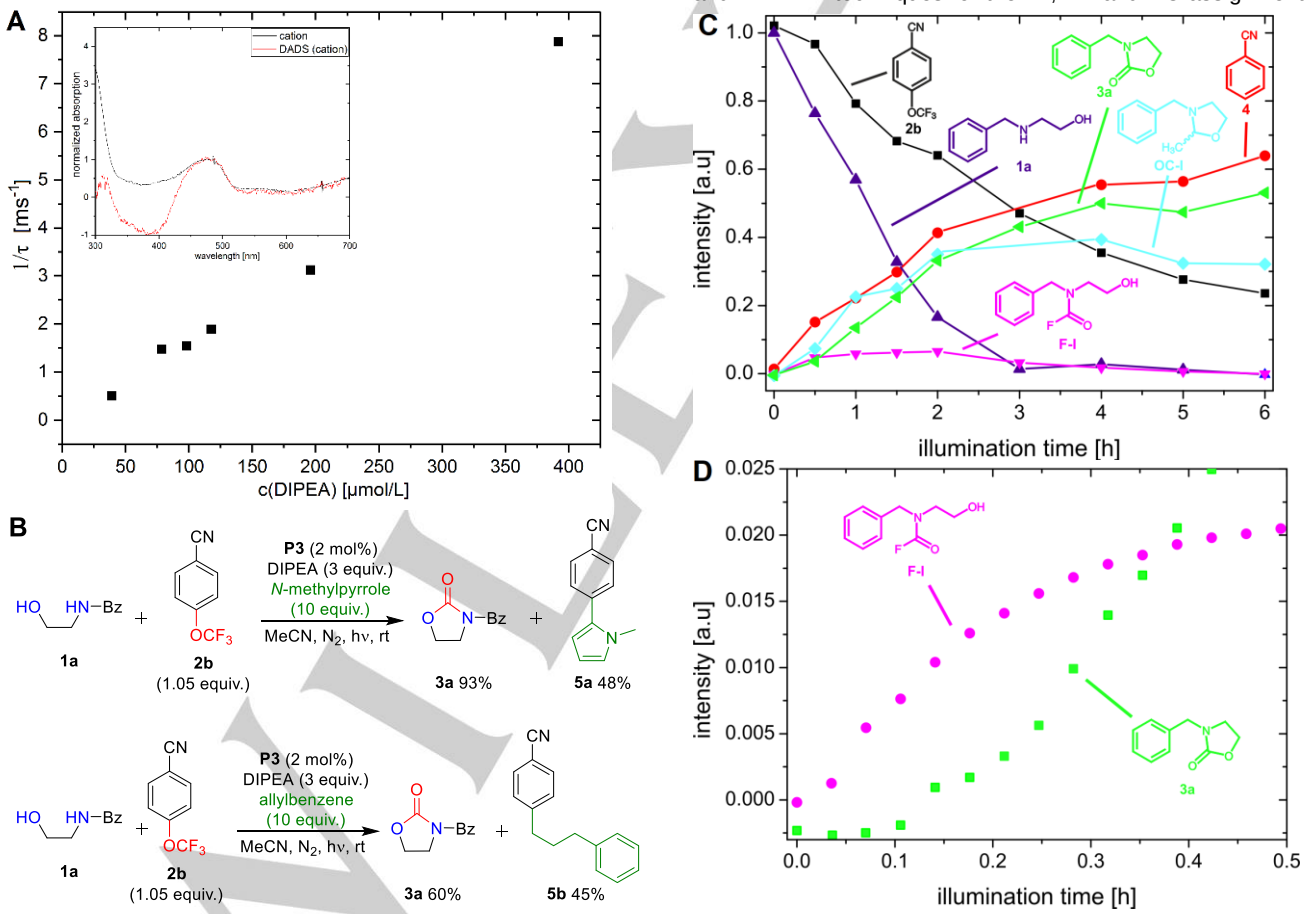

Figure 2. a) Stern-Volmer plot of quenching of the **P3** radical cation with DIPEA; inset: comparison of **P3** radical cation spectrum obtained *via* transient spectroscopy and spectro-electro chemistry (See SI for details). **b)** Radical trapping experiments with *N*-methylpyrrole and allylbenzene. **c)** *Ex situ* reaction profile of **1a** (100 mM), **2b** (105 mM), **P3** (2 mM) and DIPEA (300 mM) in CD_3CN. Next to the major products **3a** (green) and **4** (red), two intermediates can be detected; **F-I** (magenta), which is the next downstream intermediate of fluorophosgene and the direct precursor of **3a** and **OC-I** (cyan). **OC-I** presents an off-cycle intermediate being in an ongoing water dependent equilibrium with **1a**. As long as fluorophosgene is generated, **OC-I** is slowly converted into **3a** through **1a**. **d)** Excerpt of the *in situ* reaction profile of **1a** (100 mM), **2b** (110 mM), **P3** (2 mM) and DIPEA (300 mM) in CD_3CN showing the initial trend of **3a** (green) and **F-I** (magenta). The formation of **3a** is preceded by an initial lag-phase whilst the intermediate **F-I** is generated immediately after the light is turned on as the direct precursor of **3a**.

intermediate was identified as a carbonyl fluoride adduct (**F-I**) of **1a**. The immediate formation of **F-I** combined with the lag-phase of **3a** in the illuminated *in situ* NMR profile (Fig. 2d) suggested **F-I** as direct precursor of **3a.** This is further solidified by the fact that once the light is turned off, a distinct conversion of **F-I** into **3a** can be observed (for spectra see SI).
In addition, a second, off-cycle intermediate (**OC-I**, Fig. 2c) could be assigned. The emergence of **OC-I** is the reason for the evidently faster decrease of **1a** with respect to **2b** (Fig. 2c), as it stems from a side reaction of **1a** with acetaldehyde, which in turn is liberated after downstream reactions from DIPEA (see SI). From the three hour mark on in Fig. 2c, it is evident, that **1a** and **F-I** are already gone, whilst **OC-I** is slowly decreasing and **1a** is still slowly increasing. This suggests that **OC- I** and **1a** are in a slow off-cycle equilibrium. It could also be shown that this equilibrium is heavily water dependent (see SI). This results in **3a** still being generated even after **1a** is fully consumed as long as fluorophosgene is still liberated. Furthermore, addition of water can effectively reduce the formation of **OC-I** and increase the reaction rates significantly (See SI for further details on the NMR analyses). Therefore, we propose the following mechanism for the liberation of fluorophosgene from **2b** (Fig. 3). **P3** is excited by the light of 400 nm LEDs. The two excited photocatalyst molecules **P3*** form a CT-complex dimer which disproportionates to the corresponding $\mathbf{P3}^{\bullet+}$ and $\mathbf{P3}^{\bullet-}$. The $\mathbf{P3}^{\bullet-}$ reduces **2b** leading to its fragmentation into the aryl radical and trifluoromethanolate. Trifluoromethanolate decomposes into F^- and fluorophosgene, which readily reacts with amine- or alcohol-based nucleophiles resulting in a carbonylfluoride intermediate (see **F-I)**.[17] Subsequent cyclization leads to the desired product. To regenerate **P3**, the $\mathbf{P3}^{\bullet+}$ oxidizes DIPEA and the aryl radical abstracts a hydrogen atom from $\text{DIPEA}^{\bullet+}$ or the solvent to give benzonitrile. Next to the main pathway, a second off-cycle pathway is in progress. Downstream reactions of DIPEA lead to the liberation of acetaldehyde, which can readily react with **1a** to yield the off-cycle intermediate **OC-I**. The resulting equilibrium of **OC-I** and **1** is heavily dependent on the water concentration. As long as fluorophosgene is provided, **OC-I** is slowly converted into **3a** through **1a**. Addition of extra water can virtually suppress the off-cycle equilibrium, which in turn accelerates the reaction.

Conclusions

In summary, we have developed the first, visible light mediated procedure for the cleavage of an aryl trifluoromethoxy ether and the controlled liberation and *in-situ* conversion of fluorophosgene for the synthesis of carbamates, carbonates and urea derivatives. The method shows regio-selectivity for aliphatic amines and/or alcohols in presence of aromatic ones. No racemization of amino acid stereocenters was observed. Transient spectroscopy suggests the formation of a catalyst CT-complex dimer as the catalytic active species. NMR measurements identified key intermediates consolidating a stepwise fragmentation into fluorophosgene as the most likely

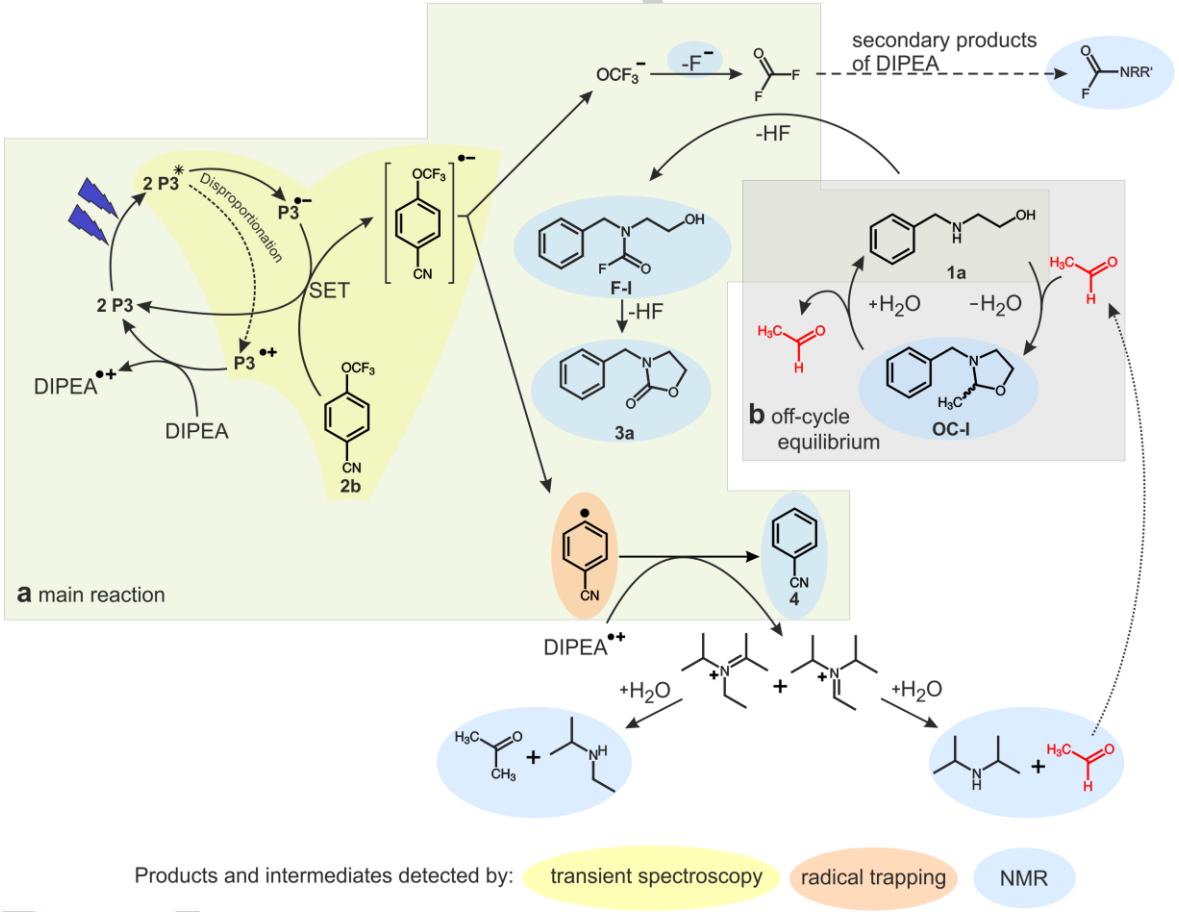

Figure 3. Proposed catalytic cycle for the photocatalytic liberation of fluorophosgene for substrate **1a**, based on the conducted mechanistic studies. The mechanism can be differentiated into two segments: **a:** The main reaction, which comprises the photocatalytic liberation of fluorophosgene by reducing **2b** and the subsequent reaction of fluorophosgene with **1a** over **F-I** to yield **3a**. **b:** The off-cycle equilibrium (gray background), which describes the water dependent equilibrium between **1a** and **OC-I** through addition and cleavage of acetaldehyde (secondary product of DIPEA). Detected products and intermediates are highlighted.

mechanistic pathway; while also uncovering a water dependent off-cycle equilibrium, which can be effectively modulated to accelerate the reaction. Notably, this method expands the toolbox of photoredoxcatalysis by the generation of an extremely reactive species which is not based on radical reactivity under mild reaction conditions.

Acknowledgements

This work was supported by the German Science Foundation (DFG) (GRK 1626, Chemical Photocatalysis). We thank Dr. Rudolf Vasold (University of Regensburg) for his assistance in GC-MS measurements and Regina Hoheisel (University of Regensburg) for her assistance in cyclic voltammetry measurements.

Conflict of interest

The authors declare no conflict of interest.

Author contributions

¶: Authors contributed equally to this work. D. P. developed the project, optimized the reaction, prepared the substrate scope and the manuscript. P. N. performed the NMR measurements and evaluations and contributed to the mechanistic part of the manuscript. F. B. Performed the transient spectroscopy experiments and evaluations. V. S. assisted with the NMR measurements. B. D., R. M. G. and B. K. supervised the project and the preparation of the manuscript.

Keywords: Photocatalysis • CT-Complex • Fluorophosgene • NMR-Spectroscopy • Trifluoromethoxyarenes

[1] (a) Heravi, M. M.; Zadsirjan, V.; Farajpour, B. *RSC Adv.* **2016**, *6*, 30498–30551; (b) Rodrigo, M. A.; Oturan, N.; Oturan, M. A. *Chem. Rev.* **2014**, *114*, 8720−8745; (c) Magano, J.; Dunetz, J. R. *Chem. Rev.* **2011**, *111*, 2177–2250; (d) Zhou, Y.; Wang, J.; Gu, Z.; Wang, S.; Zhu, W.; Aceña, J. L.; Soloshonok, V. A.; Izawa, K.; Liu, H. *Chem. Rev.* **2016**, *116*, 422−518.

[2] (a) Ghosh, A. K.; Brindisi, M. *J. Med. Chem.* **2015**, *58*, 2895−2940; (b) Parrish, J. P.; Salvatore, R. N.; Jung, K. W. *Tetrahedron* **2000**, *56*, 8207–8237; (c) Díaz, D. J.; Darko, A. K.; McElwee-White, L. *Eur. J. Org. Chem.* **2007**, 4453–4465.

[3] Pasquato, L.; Modena, G.; Cotarca, L.; Delogu, P.; Mantovani, S. *J. Org. Chem.* **2000**, *65*, 8224–8228.

[4] (a) W. Schneider, W. Diller in *Ullmann's Encyclopedia of Industrial Chemistry*, Vol. 26, Wiley-VCH: Weinheim, **2000**, pp 623−632 (b) Cotarca, L.; Geller, T.; Répási, J. *Org. Process Res. Dev.* **2017**, *21*, 1439−1446.

[5] Sakakura, T.; Kohnoa, K. *Chem. Commun.* **2009**, 1312–1330.

[6] Romero, N. A.; Nicewicz, D. A. *Chem. Rev.* **2016**, *116*, 10075–10166.

[7] (a) Petzold, D.; König, B. *Adv. Synth. Catal.* **2018**, *360*, 626–630; (b) Ghosh, I.; Ghosh, T.; Bardagi, J. I.; König, B. *Science* **2014**, *346*, 725–728; (c) Ghosh, I.; König, B., *Angew. Chem. Int. Ed.* **2016**, *55*, 7676–7679; (d) Düsel, S. J. S.; König, B *J. Org. Chem*. **2018**, *83*, 7676; (e) Romero, N. A.; Margrey, K. A.; Tay, N. E.; Nicewicz, D. A. *Science* **2015**, *349*, 1326–1330.

[8] (a) Twilton, J.; Le, C.; Zhang; P. Shaw, M. H.; Evans, R. W.; MacMillan, D. W. C., *Nat. Rev.* **2017**, *1*, 52; (b) Seo, H.; Katcher, M. H.; Jamison, T. F. *Nat. Chem.* **2017**, *9*, 453–456; (c) Studer, A.; Curran, D. P. *Nat. Chem.* **2014**, *6*, 765–773; (d) Hopkinson, M. N.; Tlahuext-Aca, A.; Glorius, F., *Acc. Chem. Res.* **2016**, *49*, 2261–2272.

[9] (a) Neubauer, A.; Grell, G.; Friedrich, A.; Bokarev, S. I.; Schwarzbach, P.; Gärtner, F.; Surkus, A.-E.; Junge, H.; Beller, M.; Kühn, O.; Lochbrunner, S. *J. Phys. Chem. Lett.* **2014**, *5*, 1355–1360; (b) Singh, A.; Fennell, C. J.; Weaver, J. D. *Chem. Sci.* **2016**, *7*, 6796–6802; (c) Lu, Z.; Yoon, T. P. *Angew. Chem. Int. Ed.* **2012**, *51*, 10329–10332.

[10] (a) Shaw, M. H.; Twilton, J.; MacMillan, D. W. C. *J. Org. Chem.* **2016**, *81*, 6898–6926; (b) Majek, M.; Jacobi von Wangelin, A. *Acc. Chem. Res.* **2016**, *49*, 2316–2327; (c) Petrone, D. A.; Ye, J.; Lautens, M. *Chem. Rev.* **2016**, *116*, 8003–8104.

[11] (a) Iijima, A.; Amii, H., *Tetrahedron Lett.* **2008**, *49*, 6013–6015; (b) Goh, K. K. K.; Sinha, A.; Fraser, C.; Young, R. D. *RSC Adv.* **2016**, *6*, 42708–42712; (c) Combellas, C., Kanoufi, F., Thiébault A. *J. Electroanal. Chem.* **1997**, *432*, 181–192.

[12] (a) Sahoo, B.; Hopkinson, M. N. *Angew. Chem. Int. Ed.* **2018**, *57*, 7942–7944; (b) Togni, A., Jelier, B. J., Tripet, P. F., Pietrasiak, E., Franzoni, I.; Jeschke, G. *Angew. Chem. Int. Ed.* 10.1002/anie.201806296

[13] (a) Pearson, R. M.; Hooi-Lim, C.; McCarthy, B. G.; Musgrave, C. B. *J. Am. Chem. Soc.* **2016**, *138*, 11399−11407; (b) Du, Y.; Pearson, R.; Hooi-Lim, C.; Sartor, S.; Ryan, M.; Yang, H.; Damrauer, N.; Miyake, G. *Chem. Eur. J.*, **2017**, *23,* 10962−10968.

[14] McCarthy, B. G.; Pearson, R. M.; Lim, C.-H.; Sartor, S.; Damrauer, N. H.; Miyake, G. M., *J. Am. Chem. Soc.* **2018**, 140, 5088–5101.

[15] Sartor, S. M., McCarthy, B. G., Pearson, R. M., Miyake, G. M.; Damrauer, N. H. *J. Am. Chem. Soc.* **2018**, *140*, 4778–4781.

[16] Hari, D. P., Schroll, P.; König, B., *J. Am. Chem. Soc.* **2012**, *134*, 2958–2961.

[17] Nguyen, M.; Matus, M. H.; Ngan, V.; Haiges, R.; Christe, K. O.; Dixon, D. A. *J. Phys. Chem. A* **2008**, *112*, 1298–1312.

10.1002/chem.201804603

WILEY-VCH

FULL PAPER

Fluorophosgene was liberated by the photocatalytic reduction of a simple aryltrifluoromethoxyether. This highly reactive species was used for the synthesis of cyclic carbonates, carbamates and urea derivatives. The reaction mechanism was investigated by an in-depth NMR study as well as cyclovoltammetry and transient spectroscopy which suggests a charge-transfer complex dimer as the catalytic active species.

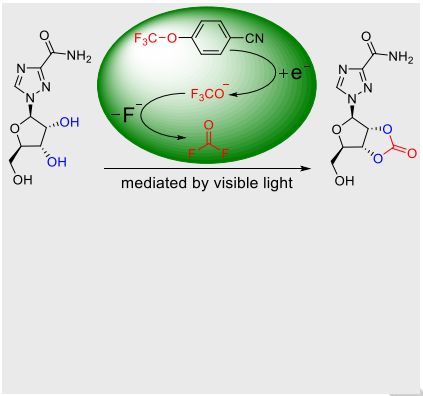

*Daniel Petzold, Philipp Nitschke, Fabian Brandl, Veronica Scheidler, Bernhard Dick, Ruth M. Gschwind, Burkhard König**

1 – 5

Visible Light Mediated Liberation and *in situ* Conversion of Fluorophosgene